




# Adaptive Processor Frequency Adjustment for Mobile Edge Computing with Intermittent Energy Supply

Tiansheng Huang , Weiwei Lin , Ying Li, Xiumin Wang, Qingbo Wu, Rui Li, Ching-Hsien Hsu ,  
and Albert Y. Zomaya , *Fellow, IEEE*

**Abstract**—With astonishing speed, bandwidth, and scale, Mobile Edge Computing (MEC) has played an increasingly important role in the next generation of connectivity and service delivery. Yet, along with the massive deployment of MEC servers, the ensuing energy issue is now on an increasingly urgent agenda. In the current context, the large scale deployment of renewable-energy-supplied MEC servers is perhaps the most promising solution for the incoming energy issue. Nonetheless, as a result of the intermittent nature of their power sources, these special design MEC server must be more cautious about their energy usage, in a bid to maintain their service sustainability as well as service standard. Targeting optimization on a single-server MEC scenario, we in this paper propose NAFA, an adaptive processor frequency adjustment solution, to enable an effective plan of the server's energy usage. By learning from the historical data revealing request arrival and energy harvest pattern, the deep reinforcement learning-based solution is capable of making intelligent schedules on the server's processor frequency, so as to strike a good balance between service sustainability and service quality. The superior performance of NAFA is substantiated by real-data-based experiments, wherein NAFA demonstrates up to 20% increase in average request acceptance ratio and up to 50% reduction in average request processing time.

**Index Terms**—Deep Reinforcement Learning, Event-driven Scheduling, Mobile edge computing, Online Learning, Semi-Markov Decision Process.



## 1 INTRODUCTION

### 1.1 Background and Motivations

LATELY, Mobile Edge Computing (MEC) has emerged as a powerful computing paradigm for the future Internet of Things (IoTs) scenarios. MEC servers are mostly deployed in proximity to the users, with the merits of seamless coverage and extremely low communication latency to the users. Also, the MEC servers feature the light-weight deployment,

enabling their potential large-scale application in various scenarios.

Despite an attractive prospect, two crucial issues might be encountered by the real application:

- 1) The large-scale deployment of grid-power MEC servers has almost exhausted the existing energy resource and resulted in an enormous carbon footprint. This in essence goes against the green computing initiative.
- 2) With millions or billions of small servers deployed amid every corner of the city, some of the locations could be quite unaccommodating for the construction of grid power facility, and even for those in a good condition, the construction and operation overhead of the power facility alone should not be taken lightly.

With these two challenges encountered during the large-scale application of MEC, we initiate an alternative usage of *intermittent energy supply*. These supplies could be *solar power*, *wind power* or *wireless power*, etc. Amid these alternatives, renewable energy, such as solar power and wind power, could elegantly address both the two concerns. The wireless power still breaches the green computing initiative, but can at least save the construction and operation cost of a complete grid power system for all the computing units.

However, all of these intermittent energy supplies reveal a nature of unreliability: power has to be stored in a battery with limited capacity for future use and this limited energy is clearly incapable of handling all the workloads when

- *The authors would like to thank the three anonymous reviewers for their constructive comments. Special thanks are due to Dr. Minxian Xu of Shenzhen Institutes of Advanced Technology, Chinese Academy of Sciences, for his constructive advice on experiment setup. This work is supported by National Natural Science Foundation of China (62072187, 61872084), Guangdong Major Project of Basic and Applied Basic Research(2019B030302002), Guangzhou Science and Technology Program key projects (202007040002, 201907010001), and Fundamental Research Funds for the Central Universities, SCUT (2019ZD26).*
- *T. Huang, W. Lin, Y. Li, and X. Wang are with the School of Computer Science and Engineering, South China University of Technology, China. Email: tianshenghuangscut@gmail.com, linww@scut.edu.cn, 1650332175@qq.com, xmwang@scut.edu.cn.*
- *CH. Hsu is with the Department of Computer Science and Information Engineering, Asia University, Taichung, Taiwan and with the Department of Computer Science and Information Engineering, Asia University, Taichung, Taiwan. Email: robertchh@gmail.com.*
- *Q. Wu is with the College of Computer, National University of Defense Technology, Changsha 410073, China. Email: wuqingbo@tj.kylinos.cn.*
- *R. Li is with Peng Cheng Laboratory, Shenzhen 518000, China. Email: lir@pcl.ac.cn.*
- *AY. Zomaya is with the School of Computer Science, The University of Sydney, Sydney, Australia. Email: albert.zomaya@sydney.edu.au.*

mass requests are submitted. With this concern, servers have two potential options to accommodate the increasing workloads:

- 1) They directly reject some of the requests (perhaps those require greater computation), in a bid to save energy for the subsequent requests.
- 2) They lower the processing frequency of their cores to save energy and accommodate the increasing workloads. Nevertheless, this way does not come without a cost: each request might suffer a prolonged processing time.

These heuristic ideas of energy conservation elicit the problem we are discussing in this paper. We are particularly interested in the potential request treatment (i.e., should we reject an incoming request, and if not, how shall we schedule the processing frequency for it) and their consequent effects on the overall system performance.

The problem could become even more sophisticated if regarding the unknown and non-stationary request arrival and energy harvest pattern. Traditional rule-based methods clearly are incompetent in this volatile context: as a result of their inflexibility, even though they might work in a particular setting (a specific arrival pattern, for example), they may not work equally well if in a completely different environment.

Being motivated, we shall design a both effective and adaptive solution that is able to cope with the uncertainty brought by the energy supply and request pattern. Moreover, the solution should be highly programmable, allowing custom design based on the operators' expectations towards different performance metrics.

## 1.2 Contributions

The major contributions of our work are presented in the following:

- 1) We have analyzed the real working procedure of an intermittent-energy-driven MEC system, based on which, we propose an event-driven schedule scheme, which is deemed much matching with the working pattern of this system.
- 2) Moreover, we propose an energy reservation mechanism to accommodate the event-driven feature. This mechanism is novel and has not been available in other sources, to our best knowledge.
- 3) Based on the proposed scheduling mechanism, we have formulated an optimization problem, which basically covers a few necessary system constraints and two main objectives: cumulative processing time and acceptance ratio.
- 4) We propose a deep reinforcement learning-based solution (NAFA) to optimize the joint request treatment and frequency adjustment action.
- 5) We do the experiments based on real solar data. By our experimental results, we substantiate the effectiveness and adaptiveness of our proposed solutions. In addition to the general results, we also develop a profound analysis of the working pattern of different solutions.

To the best knowledge of the authors, our main focus on event-driven scheduling for an intermittent energy-supplied system has not been presented in other sources. Also, our proposed solution happens to be the first trackable deep reinforcement learning solution to an SMDP model. It has the potential to be applied to other network systems that follow a similar event-driven working pattern. In this regard, we consider our novel work as a major contribution to the field.

## 2 RELATED WORK

### 2.1 AI-driven techniques and their application in MEC

AI-driven algorithms have been broadly studied thanks to their attractive efficiency and flexibility. In many fields, such as service orchestration [1], vehicular or industrial IoT networks (see [2], [3]), crowdsensing (see [4], [5]), etc, lines of research on AI application have been conducted. The proposed AI-driven algorithms all achieved significant performance enhancement, comparing with traditional methodology. Among these emerging topics, AI-driven MEC can be regarded as one of the hottest agenda. To illustrate, in [6], Chen *et al.* combined the technique of Deep Q Network (DQN) with a multi-object computation offloading scenario. By maintaining a neural network inside its memory, the MU is enabled to intelligently select an offloading object among the accessible base stations. Wei *et al.* in [7] introduced a reinforcement learning algorithm to address the offloading problem in the IoT scenario, based on which, they further proposed a value function approximation method in an attempt to accelerate the learning speed. In [8], Min *et al.* further considered the privacy factors in healthcare IoT offloading scenarios and proposed a reinforcement learning-based scheme for a privacy-ensured data offloading.

Refs. [6]–[9] mentioned above are all based on Markov Decision Process (MDP), in which the action scheduling is performed periodically based on a fixed time interval. However, in the real scenario, the workflow of an agent (server or MU) is usually event-driven. To be specific, the agent is supposed to promptly make the scheduling and perform actions once an event has occurred (e.g. a request arrives) but not wait until a fixed periodicity is met.

### 2.2 Event-Driven SMDP

Motivated by the gap between current research and the agent's real working pattern, we consider the Semi-Markov Decision Process (SMDP) as our basic model instead. Unlike the conventional MDP model, for an SMDP model, the time interval between two sequential actions does not necessarily need to be the same. As such, it is super matching for an event-triggered schedule, like the one we need for the requests scheduling.

SMDP is a powerful modeling tool that has been applied to many fields, such as wireless networks, operation management, etc. In [10], Zheng *et al.* first applied SMDP in the scenario of vehicular cloud computing systems. A discounted reward is adopted in their system model, based on which, the authors further proposed a value iteration method to derive the optimal policy. In [11], SMDP is first applied to energy harvesting wireless networks. For problem-solving, the authors adopted a model-based policy

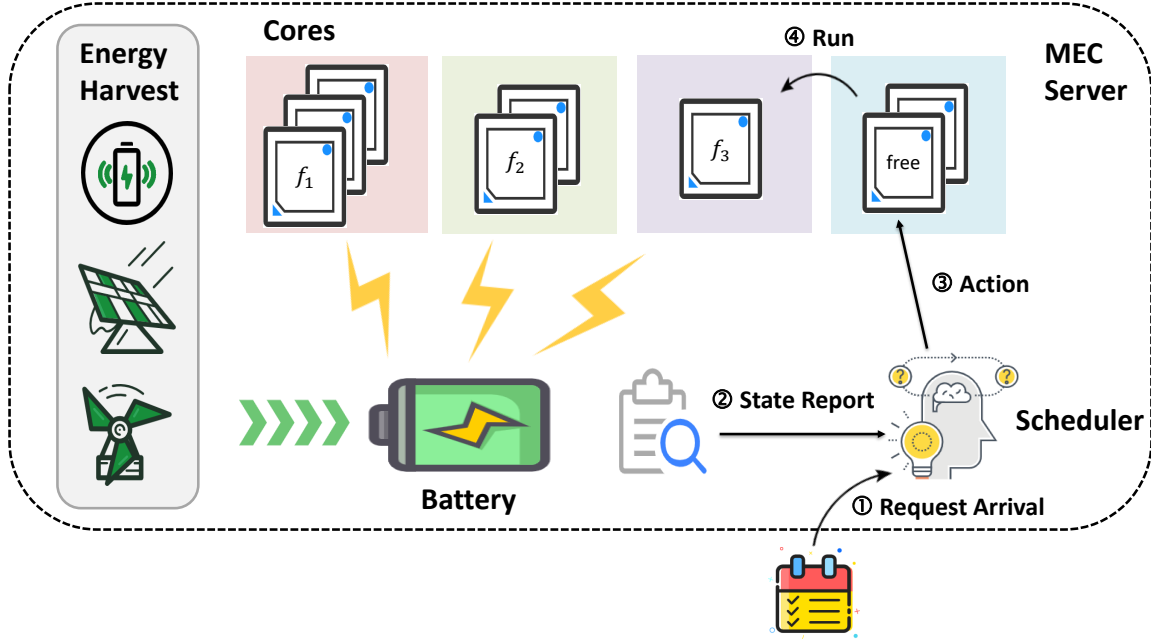


Fig. 1: System architecture for an intermittent-energy-supplied MEC system.

iteration method. However, the model-based solution proposed in the above work can not address the problem when the state transition probability is unknown, and in addition, it cannot deal with the well-known curse-of-dimensionality issue.

To fix the gap, based on an SMDP model that is exclusively designed for an NB-IOT Edge Computing System, Lei *et al.* in [12] further proposed a reinforcement learning-based algorithm. However, the proposed algorithm is still too restricted and cannot be applied in our current studied problems, since several assumptions (e.g., exponential sojourn time between events) must be made in advance. Normally, these assumptions are inevitable for the derivation of state-value or policy-value estimation in an SMDP model, but unfortunately, could be the main culprit leading to great divergence between theory and reality.

As a result, we in this paper will **jettison all the assumptions** typically presented in an SMDP formulation. Alternatively, we adopt a Double Deep Q Network (DDQN) (see [13]) to predict the state-action value function and to derive a near-optimal policy based on which. Our method is a more general solution for an SMDP model and is designed mostly based on a practical and usable standpoint.

### 3 PROBLEM FORMULATION

#### 3.1 System Overview

In this paper, we target the optimization problem in a multi-users single-server MEC system that is driven by intermittent energy supply (e.g., renewable energy, wireless charging). As depicted in Fig. 1, multiple central processing units (CPUs) and a limited-capacity battery, together with communication and energy harvesting modules, physically constitute an MEC server. Our proposed MEC system makes

scheduling on requests following an event-driven workflow, i.e., our request scheduling process is evoked immediately once a request is collected. This event-driven process can be specified by the following steps:

- 1) Collect the request and check the current system status, e.g., battery and energy reservation status and CPU core status.
- 2) Do schedule to the incoming request based on its characteristic and current system status. Explicitly, the scheduler is supposed to make the following decisions:
  - a) Decide whether to accept the request or not.
  - b) If accepted, decide the *processing frequency* of the request. We refer to *processing frequency* as the frequency that a CPU core might turn to while processing this particular request. The scheduler should not choose the frequency that might potentially *over-reserve* the currently available energy or *over-load* the available cores.
- 3) Do energy reservation for the request based on the decided frequency. A CPU core cannot use more than the reserved energy to process this request.
- 4) The request is scheduled to the corresponding CPU core and start processing.

Given that the system we study is **not** powered by reliable energy supply (e.g., coal power), a careful plan of the available energy is supposed to be made in order to promote the system performance.

#### 3.2 Formal Statement

In this subsection, we shall formally introduce the optimization problem by rigorous mathematics formulation (key no-

TABLE 1: Key notations for problem formulation

Notations	Meanings
$a_i$	action scheduled for the $i$ -th request
$f_n$	$n$ -th processing frequency option (GHz)
$d_i$	data size of the $i$ -th request (bits)
$\nu$	computation complexity per bit
$\kappa$	effective switched capacitance
$m$	number of CPU cores
$\tau_{a_i}$	processing time of the $i$ -th request
$e_{a_i}$	energy consumption of the $i$ -th request
$B_i$	battery status when $i$ -th request arrives
$B_{max}$	maximum battery capacity
$\lambda_{i,i+1}/\rho_{i,i+1}$	captured/consumed energy between arrivals of the $i$ -th and $(i+1)$ -th request
$S_i$	reserved energy when $i$ -th request arrives
$\Psi_i$	number of working CPU cores when the $i$ -th request arrives
$\eta$	tradeoff parameter

tations and their meanings are given in Table 1). We consider the optimization problem for an MEC server with  $m$  CPU cores, all of whose frequency can be adaptively adjusted via Dynamic Voltage and Frequency Scaling (DVFS) technique. Then we first specify the "action" for the optimization problem.

### 3.2.1 Action

The decision (or action) in this system specifies the treatment of the incoming request. Explicitly, it specifies 1) whether to accept the request or not, 2) the processing frequency of the request. Formally, let  $i$  index an incoming request by its arrival order. The action for the  $i$ -th request is denoted by  $a_i$ . Explicitly, we note that:

- 1)  $a_i \in \{0, 1, \dots, n\}$  denotes the action index of the CPU frequency at which the request is scheduled, where  $n$  represents the maximum index (or total potential options) for frequency adjustment. For option  $n$ ,  $f_n$  GHz frequency will be scheduled to the request.
- 2) Specially, when  $a_i = 0$ , the request will be rejected immediately.

### 3.2.2 Processing Time and Energy Consumption

The action we take might have a direct influence on the request *processing time*, which can be specified by:

$$\tau_{a_i} = \begin{cases} \frac{\nu \cdot d_i}{f_{a_i}} & a_i \in \{1, \dots, n\} \\ 0 & a_i = 0 \end{cases} \quad (1)$$

where we denote  $d_i$  as the processing data size of an offloading request,  $\nu$  as the required CPU cycles for computing one bit of the offloading data. Without loss of generality, we assume  $d_i$ , i.e., processing data size, as a stochastic variable while regarding  $\nu$ , i.e., required CPU cycles per bit, fixed for all requests.

Also, by specifying the processing frequency, we can derive the *energy consumption* for processing the request,

which can be given as:

$$e_{a_i} = \begin{cases} \kappa f_{a_i}^2 \cdot \nu \cdot d_i & a_i \in \{1, \dots, n\} \\ 0 & a_i = 0 \end{cases} \quad (2)$$

where we denote  $\kappa$  as the effective switched capacitance of the CPUs.

### 3.2.3 Battery Status

Recall that the MEC server is driven by intermittent energy supply, which indicates that the server has to store the captured energy in its battery for future use. Concretely, we shall introduce a virtual queue, which serves as a measurement of the server's current battery status. Formally, we let a virtual queue, whose backlog is denoted by  $B_i$ , to capture the energy status when the  $i$ -th request arrives.  $B_i$  evolves following this rule:

$$B_{i+1} = \min \{B_i + \lambda_{i,i+1} - \rho_{i,i+1}, B_{max}\} \quad (3)$$

Here,

- 1)  $\lambda_{i,i+1}$  represents the amount of energy that was captured by the server between the arrivals of the  $i$ -th and  $(i+1)$ -th request.
- 2)  $\rho_{i,i+1}$  is the consumed energy during the same interval. It is notable that the consumed energy i.e.,  $\rho_{i,i+1}$ , is highly related to the frequency of the current running cores, due to which, is also relevant to the past *actions*, regarding the fact that it is the past actions that determine the frequency of the current running cores.
- 3)  $B_{max}$  is the maximum capacity of the battery. we use this value to cap the battery status since the maximum energy status could not exceed the full capacity of the server's battery.

### 3.2.4 Energy Reservation Status

Upon receiving each of the coming requests, we shall reserve the corresponding amount of energy for which so that the server could have enough energy to finish this request. This reservation mechanism is essential in maintaining the stability of our proposed system.

To be specific, we first have to construct a virtual queue to record the *energy reservation status*. The energy reservation queue, with backlog  $S_i$ , evolves between request arrivals following this rule:

$$S_{i+1} = \max \{S_i + e_{a_i} - \rho_{i,i+1}, 0\} \quad (4)$$

where  $\rho_{i,i+1}$  is the consumed energy (same definition in Eq. (3)) and  $e_{a_i}$  is the energy consumption for the  $i$ -th request (same definition in Eq. (2)). By this means,  $S_{i+1}$  exactly measures how much energy has been reserved by the 1-th to the  $i$ -th request<sup>1</sup>.

1. Some may wonder the rationale behind the subtraction of  $\rho_{i,i+1}$ . Considering the case that in a specific timestamp (e.g., the timestamp that the  $i$ -th request arrives), the processing of a past request (e.g., the  $(i-1)$ -th request) could be unfinished, but have already consumed some of the reservation energy. Then, the reservation energy for it should subtract the already consumed part.

### 3.2.5 Energy Constraint

By maintaining the *energy reservation status*, we can specify *energy constraint* to control the action when the energy has already been full-reserved. The constraint can be given as follows:

$$S_i + e_{a_i} \leq B_i \quad (5)$$

By this constraint, we ensure that the request has to be rejected if not enough energy (that has not been reserved) is available.

### 3.2.6 Resource Constraint

Recall that we assume a total number of  $m$  CPU cores are available for request processing. When the computation resources have already been full-loaded, the system has no option but to reject the arrived requests. So, we introduce the following constraint:

$$\Psi_i + \mathbb{I}\{a_i \neq 0\} \leq m \quad (6)$$

where  $\Psi_i$  denotes the number of currently working CPU cores. By this constraint, we ensure that the server could not be overloaded by the accepted request.

### 3.2.7 Optimization Problem

Now we shall formally introduce the problem that we aim to optimize, which is given as follows:

$$(P1) \quad \begin{aligned} \text{Obj1:} \quad & \min_{\{a_i\}} \sum_{i=1}^{\infty} \tau_{a_i} \\ \text{Obj2:} \quad & \max_{\{a_i\}} \sum_{i=1}^{\infty} \mathbb{I}\{a_i \neq 0\} \\ \text{C1:} \quad & S_i + e_{a_i} \leq B_i \\ \text{C2:} \quad & \Psi_i + \mathbb{I}\{a_i \neq 0\} \leq m \end{aligned} \quad (7)$$

There are two objectives that we need to consider in this problem: 1) the first objective is the cumulative *processing time* of the system, 2) and the second objective is the cumulative *acceptance*. Besides, two constraints, i.e., *Energy Constraint* and *Resource Constraint*, have been covered in our system constraints.

Obviously,  $P1$  is unsolvable due to the following facts:

- 1) **Existence of stochastic variables.** Stochastic variables, e.g.,  $d_i$  (data size of requests),  $\lambda_{i,i+1}$  (energy supplied) and request arrival rate, persist in  $P1$ .
- 2) **Multi-objective quantification.** The two objectives considered in our problem are mutually exclusive and there is not an explicit quantification between them.

To bridge the gap, we 1) set up a tradeoff parameter to balance the two objectives and transform the problem into a single objective optimization problem, 2) transform the objective function into an expected form. This leads to our newly formulated  $P2$ :

$$(P2) \quad \begin{aligned} \max_{\{a_i\}} \quad & \sum_{i=1}^{\infty} \mathbb{E} [\mathbb{I}\{a_i \neq 0\} - \eta \tau_{a_i}] \\ \text{C1:} \quad & S_i + e_{a_i} \leq B_i \\ \text{C2:} \quad & \Psi_i + \mathbb{I}\{a_i \neq 0\} \leq m \end{aligned} \quad (8)$$

where  $\eta$  serves as the tradeoff parameter to balance cumulative *acceptance* and cumulative *processing time*.  $P2$  is more concrete after the transformation, but still, we encounter the following challenges when solving  $P2$ :

- 1) **Exact constraints.** Both C1 and C2 are exact constraints that should be strictly restricted for each request. This completely precludes the possibility of applying an offline deterministic policy to solve the problem, noticing that  $B_i$ ,  $S_i$  in C1 and  $\Phi_i$  in C2 are all stochastic for each request.
- 2) **Unknown and non-stationary supplied pattern of energy.** The supplied pattern of intermittent energy is highly discrepant, varying from place to place and hour to hour<sup>2</sup>. As such, the stochastic process  $\lambda_{i,i+1}$  in Eq. (3) may not be stationary, i.e.,  $\lambda_{i,i+1}$  samples from an ever-changing stochastic distribution that is relevant with request order  $i$ , and moreover, it is unknown to the scheduler.
- 3) **Unknown and non-stationary arrival pattern.** The arrival pattern of the request's data size is unknown to the system, and also, could be highly discrepant at temporal scales.
- 4) **Unknown stochastic distribution of requests' data size.** The processing data size could vary between requests and is typically unknown to the scheduler.
- 5) **Coupling effects of actions between requests.** The past actions towards an earlier request might have a direct effect on the later scheduling process (see the evolvement of  $S_i$  and  $B_i$ )

Regarding the above challenges, we have to resort to an online optimization solution for problem-solving. The solution is expected to learn the stochastic pattern from the historical knowledge, and meanwhile, can strictly comply with the system constraint.

## 4 DEEP REINFORCEMENT LEARNING-BASED SOLUTION

### 4.1 Formulation of a Semi-Markov Decision Process

To develop our reinforcement learning solution, we shall first transform the problem into an *Semi-Markov Decision Process* (SMDP) formulation. In our SMDP formulation, we assume the system *state* as the system running status when a request has come, or, when the scheduler is supposed to take *action*. After an action being taken by the scheduler, a *reward* would be achieved, and the state (or system status) correspondingly transfers. It follows an *event-driven* process, that is, the scheduler decides the action once a request has come but does nothing while awaiting. And as a result, the time interval between two sequential actions may not be the same. This is the core characteristic for an SMDP model and is the major difference from a normal MDP model.

Now we shall specify the three principal elements (i.e., states, action, and rewards) in our SMDP formulation in sequence, and please note that most of the notations we used henceforth are consistent with those in Section 3.

2. Considering the energy harvest pattern of solar power. We have a significant difference in harvest magnitude between day and night.

#### 4.1.1 System States

A system state is given as a tuple:

$$s_i \triangleq \{T_i, B_i, S_i, \psi_{i,1}, \dots, \psi_{i,n}, d_i\} \quad (9)$$

Explicitly,

- 1)  $T_i$  is the **24-hour-scale local time** when the  $i$ -th request arrives in the MEC server. We incorporate this element in our state in order to accommodate the temporal factor that persists in the energy and request pattern.
- 2)  $B_i$  is the **battery status**, same as we specify in Eq. (3).
- 3)  $S_i$  is the **energy reservation status**, same as we specify in Eq. (4).
- 4)  $\psi_{i,n}$  denotes the **running CPU cores in the frequency of  $f_n$  GHz**. Meanwhile, it is intuitive to see that  $\Psi_i = \sum_{n=1}^n \psi_{i,n}$  where  $\Psi_i$  is the total running cores we specify in Eq. (6).
- 5)  $d_i$  is the **data size** of the  $i$ -th request.

Information captured by a state could be comprehended as the current system status that might support the action scheduling of the incoming  $i$ -th request. More explicitly, we argue that the formulated states should at least cover the system status that helps construct a *possible action set*, but could cover more types of informative knowledge to support the decision (e.g.,  $T_i$  in our current formulation, which will be formally analyzed later). The concept of *possible action set* would be given in our explanation of *system actions*.

#### 4.1.2 System Actions

Once a request arrives, given the current state (i.e., the observed system status), the scheduler is supposed to take action, deciding the treatment of the request. Indicated by the system constraints C1 and C2 in P2, we are supposed to make a restriction on the to-be taken action. By specifying the states (or observing the system status), it is not difficult to find that we can indeed get a closed-form possible action set, as follows:

$$a_i \in \mathcal{A}_{s_i} \triangleq \{a | \Psi_i + \mathbb{I}\{a \neq 0\} \leq m, S_i + e_a \leq B_i\} \quad (10)$$

where  $\Psi_i$ ,  $B_i$  and  $S_i$  are all covered in our state formulation. By taken action from the defined possible action set, we address challenge 1) **exact constraints**, that we specify in P2.

#### 4.1.3 System Rewards

Given state and action, a system reward will be incurred, in the following form:

$$r(s_i, a_i) = \mathbb{I}\{a_i \neq 0\} - \eta\tau_{a_i} \quad (11)$$

The reward of different treatments of a request is consistent with our objective formulation in P2 (see Eq. (8)). The goal of our MDP formulation is to maximize the expected achieved rewards, which means that we aim to maximize  $\sum_{i=1}^{\infty} \mathbb{E}[\mathbb{I}\{a_i \neq 0\} - \eta\tau_{a_i}]$ , the same form with the objective in P2. Besides, here we can informally regard  $\mathbb{I}\{a_i \neq 0\}$  as a "real reward" of accepting a request and  $\tau_{a_i}$  as the "penalty" of processing a request.

#### 4.1.4 State Transferred Probability

After an action being taken, the state will be transferred to another one when the next arrival of the request occurs. The state transferred probability to a specific state is assumed to be *stationary* given the current state and the current action, i.e., we assume that:

$$p(s_{i+1} | s_i, a_i) = \text{constant} \quad (12)$$

This assumption is the core part in our MDP formulation. And this is our main motivation to cover  $T_i$  and  $\psi_{i,1}, \dots, \psi_{i,n}$  (rather than  $\Psi_i$ ) in our state formulation. After all, we hope that the the state transferred probability, i.e.,  $p(s_{i+1} | s_i, a_i)$  is indeed a constant.

Explicitly, by given  $a_i$ ,  $T_i$ ,  $\psi_{i,1}, \dots, \psi_{i,n}$  and  $d_i$ , we expect the probability that  $s_i$  transfers to  $s_{i+1}$  are a fixed constant. To reach this goal, given  $s_i$ , we need to make sure that the corresponding elements (e.g.,  $B_{i+1}$ ,  $S_{i+1}$  and  $\psi_{i+1,1}, \dots, \psi_{i+1,n}$ ) in state  $s_{i+1}$  follows the a same joint *stationary distribution*. A *stationary distribution* means it is no longer relevant with request order  $i$  if given  $s_i$ . To show this desirable property, we first need to show that:

**Observation 1 (Stationary Energy Arrival Given State).** *By specifying  $T_i$ , the captured energy between two sequential requests (i.e.,  $\lambda_{i,i+1}$ ) can be roughly regarded as samples from a stationary distribution, i.e., value of r.v.  $\lambda_{i,i+1}$  is not relevant with  $i$  (order of request) given  $T_i$ .*

*Remark.* This assumption is derived from our experience: many intermittent energy supply sources, such as solar power, wind power, have a clear diurnal pattern, but if we fix the time to a specific timestamp in a day, the energy harvest can roughly be regarded as samples from a fixed distribution. Informally, we assume a fixed energy harvest rate for a fixed timestamp, e.g., 1000 Joules/s harvest rate in 3:00 pm. And this distribution is no longer relevant with  $i$ . In this way, we respond to the non-stationary issue in challenge 2), **unknown and non-stationary supplied pattern of energy**, that we previously proposed below P2. Similarly, one can easily extend the state formulation by covering more system status (e.g., the location of the MEC server, if we aim to train a general model for multiple MEC servers scenario) to yield a more accurate estimation.

**Observation 2 (Stationary Request Arrival Given State).** *By specifying  $T_i$ , the time interval between request arrival should also be considered as samples from a stationary distribution (though still unknown). This means that the time interval between two arrivals (denoted by  $t_{i,i+1}$ ) is no longer relevant with  $i$  if given  $T_i$ .*

*Remark.* By this state formulation, we address the non-stationary issue in challenge 3), **unknown and non-stationary arrival pattern**, that we previously proposed below P2.

**Observation 3 (Stationary Energy Consumption Given State).** *By specifying  $a_i$ ,  $\psi_{i,1}, \dots, \psi_{i,n}$  and a stationary time interval between two arrivals, the consumed energy between two requests (i.e.,  $\rho_{i,i+1}$ ) could roughly be regarded as samples from a stationary distribution.*

*Remark.* Our explanation for observation 3 is that the con-

summed energy  $\rho_{i,i+1}$  is actually determined by current CPU frequency as well as the time interval between requests (i.e.,  $t_{i,i+1}$ ). Explicitly, we can roughly estimate that  $\rho_{i,i+1} = \sum_{n'=1}^n (\psi_{i,n'} + \mathbb{I}\{a_i = n'\}) t_{i,i+1}$ . But this calculation is not 100% accurate since the CPU could have slept before arrival of next request, as a result of the process finishing of a request. As a refinement, we further assume  $\rho_{i,i+1} = \sum_{n'=1}^n (\psi_{i,n'} + \mathbb{I}\{a_i = n'\}) \cdot t_{i,i+1} - y(a_i, \psi_{i,1}, \dots, \psi_{i,n}, t_{i,i+1})$  where  $y(a_i, \psi_{i,1}, \dots, \psi_{i,n}, t_{i,i+1})$  is a stochastic noise led by the halfway sleeping of CPU cores. Without loss of generality,  $y(a_i, \psi_{i,1}, \dots, \psi_{i,n}, t_{i,i+1})$  is assumed to be samples from a stationary distribution given  $a_i, \psi_{i,1}, \dots, \psi_{i,n}$  and  $t_{i,i+1}$ . By this assumption, we state that  $\rho_{i,i+1}$  is stationary if given  $a_i, \psi_{i,1}, \dots, \psi_{i,n}$  and a stationary  $t_{i,i+1}$ .

**Observation 4 (Stationary Battery and Reserved status Given State).** *By specifying  $s_i$  and  $a_i$ ,  $B_{i+1}$  and  $S_{i+1}$  can roughly be regarded as samples from two stationary distributions.*

*Remark.* See Eqs. (3) and (4), we find that  $B_{i+1}$  and  $S_{i+1}$  are relevant with  $\lambda_{i,i+1}$ ,  $\rho_{i,i+1}$ ,  $e_{a_i}$  and  $s_i$ . As per Observation 1 and 3,  $\lambda_{i,i+1}$  and  $\rho_{i,i+1}$  are all stationary given  $s_i$  and  $a_i$ . In addition, we note that  $e_{a_i}$  is stationary given the same condition since  $d_i$  is assumed to be samples from a stationary distribution and there is not other stochastic factor in Eq. (2).

**Observation 5 (Stationary Core Status Given State).** *By specifying  $s_i$  and  $a_i$ ,  $\psi_{i+1,1}, \dots, \psi_{i+1,n}$  can roughly be regarded as samples from a stationary distribution.*

*Remark.* Here we simply regard that  $\psi_{i+1,n} = \psi_{i,n} + \mathbb{I}\{a_i = n'\} - z(\psi_{i,n}, t_{i,i+1})$  where  $z(\psi_{i,n}, t_{i,i+1})$  denotes the reduction on number of active core in  $f_n$  GHz during  $t_{i,i+1}$  interval. Instinctively, we feel that the reduction, i.e.,  $z(\psi_{i,n}, t_{i,i+1})$  should at least have some sort of bearing with the running core status, i.e.,  $\psi_{i,n}$  and the time interval between requests i.e.,  $t_{i,i+1}$ . Informally, we might simply imagine that for each time unit, the amount of  $\alpha_n \cdot \psi_{i,n}$  expected reduction would be possibly incurred, where  $\alpha_n$  should be only relevant to the evaluated core frequency (i.e.,  $f_n$ ). Then, following this strand of reasoning,  $z(\psi_{i,n}, t_{i,i+1})$  should be a stochastic variable and it can be roughly regarded as samples from a stationary distribution if given  $\psi_{i,n}$  and  $t_{i,i+1}$ .

**Observation 6 (Stationary Time and Data Size Given State).** *By specifying  $s_i$  and  $t_{i,i+1}$ , the timestamp in which the next request comes, i.e.,  $T_{i+1} = T_i + t_{i,i+1}$  is naturally stationary. Besides, the data size of a request, i.e.,  $d_{i+1}$  is naturally assumed to be samples from a stationary distribution (i.e., not relevant with the arrival order  $i$ ).*

Combining Observation 4, 5 and 6, we roughly infer that there should be a unique constant specifying the transferred probability from a state to another. However, we note that this conclusion is not formal in a very rigorous sense (and it does not necessarily to be!), given the complexity that exists in the analysis as well as the **not necessarily 100% correct** assumptions we make in the observation. Our real intention of discussing the stationary property is actually to render the readers an instruction about state formulation, and show that how to extend the state if in a different application case.

#### 4.1.5 Example

In this section, we shall show the readers a simplified working procedure of our proposed SMDP model. As shown in Fig. 2, we consider three possible frequency adjustment options for each incoming request, i.e.,  $a_i \in \{0, 1, 2, 3\}$  where action  $a_i = 0$  means rejection and actions  $a_i = 1, 2, 3$  respectively correspond to a frequency setting of  $f_1, f_2, f_3$ . Our example basically illustrates the following workflows:

- 1) Before the 1-st request's arrival, a specific amount of energy (i.e., **acquired energy**, represented by the green bar) has been collected by the energy harvest modules. Then, at the instance of the 1-st request's arrival, the scheduler decides to take action  $a_1 = 1$  based on the current state<sup>3</sup>. Once the action is being taken, a) a sleeping core would waken and started to run in the frequency of  $f_1$ , b) a specific amount of energy would be reserved for processing of this request, c) and the acquired energy would be officially deemed as **stored energy**. Correspondingly, the state instantly transfers to a virtual **post-action state**, i.e., a) the first bit in core status (i.e. running core in the frequency of  $f_1$ ) would be correspondingly flipped to 1, b) the reserved energy would be updated, c) and the newly acquired energy would be absorbed into the stored energy.
- 2) Then, the state (i.e., the system status) continues to evolve over time: the running cores continuously consume the reserved energy and the stored energy (same amount would be consumed for reserved energy and stored energy). The evolvment of state pauses when the second request arrives. After observing the current system status (i.e., current state), the scheduler makes an action  $a_2 = 2$  at this time and the state similarly transfers to the post-action state.
- 3) Again, after the action being taken, the state evolves over time, and within this time interval, a core (in frequency  $f_1$ ) has finished its task. Predictably, when the 3-rd request arrives, a state with core status  $(0, 1, 0)$  would be observed, and since the available energy (sum of acquired energy and stored energy) is not sufficient for processing this request, the scheduler has no choice but to reject the request, which makes  $a_3 = 0$ . This time, the post-action state does not experience substantial change compared with the observed state (except that acquired energy has been absorbed).
- 4) The same evolvment continues and the same action and state transformation process would be repeated for the later requests.

Please note that in our former formulation, we do not involve the consideration of post-action state, since we only care about the state transformation between two formal states  $s_i$  and  $s_{i+1}$ . We present the concept of post-action

<sup>3</sup>Note that in our formal state formulation (see Eq. (9)), we do not distinguish between **acquired energy** and **stored energy**, but only interest in the **battery status**, which is the sum of these two terms. We make this distinction in this example mainly to support our illustration of the key idea.



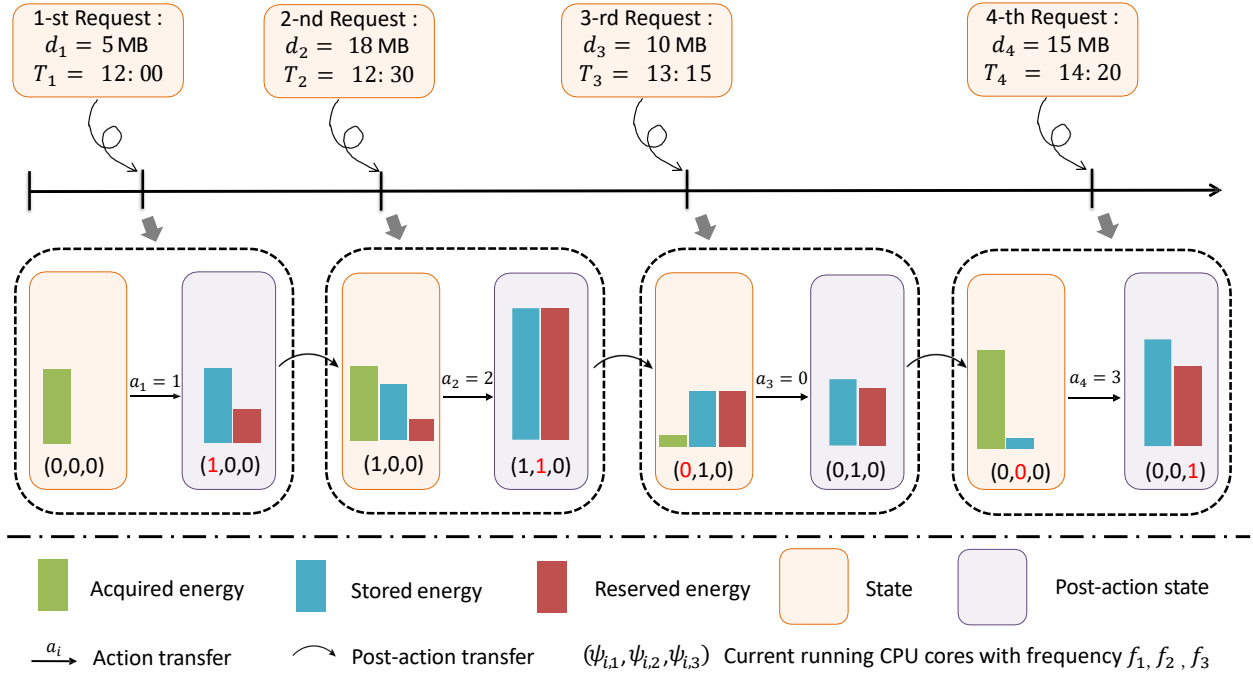


Fig. 2: Illustration of the event-driven SMDP model

state here mainly in a bid to render the readers a whole picture about how the system states might evolve over time.

## 4.2 State-Action Value Function

Recall that our ultimate goal is to maximize the expected cumulative reward, which means that we need to find a deterministic *optimal policy*  $\tilde{\pi}^*$  such that:

$$\tilde{\pi}^* = \arg \max_{a \in \mathcal{A}_s} \tilde{Q}_{\tilde{\pi}^*}(s, a) \quad (13)$$

where

$$\begin{aligned} & \tilde{Q}_{\tilde{\pi}}(s, a) \\ &= \mathbb{E}_{s_2, s_3, \dots} \left[ r(s_1, a_1) + \sum_{i=2}^{\infty} r(s_i, \tilde{\pi}(s_i)) \mid s_1 = s, a_1 = a \right] \end{aligned} \quad (14)$$

represents the expected cumulative rewards, starting from an initial state  $s$  and an initial action  $a$ .  $\tilde{\pi}^*$  is a deterministic policy that promises us the best action in cumulating expected rewards. However, it is intuitive to find that  $\tilde{Q}_{\tilde{\pi}}(s, a)$  is not a convergence value no matter how the policy  $\pi$  is defined (see the summation function), which makes it meaningless to derive  $\pi^*$  in this form.

To address this issue, we alternatively define a *discounted expected cumulative rewards*, in the following form:

$$\begin{aligned} & Q_{\pi}(s, a) \\ &= \mathbb{E}_{s_2, s_3, \dots} \left[ r(s_1, a_1) + \sum_{i=2}^{\infty} \beta^{i-1} r(s_i, \pi(s_i)) \mid s_1 = s, a_1 = a \right] \end{aligned} \quad (15)$$

where  $0 < \beta < 1$  is the discount factor and  $s$  is an initial state.

And we instead need to find a *near-optimal policy*  $\pi^*$  such that:

$$\pi^*(s) = \arg \max_{a \in \mathcal{A}_s} Q_{\pi^*}(s, a) \quad (16)$$

where  $s$  is an initial state.  $Q_{\pi}(s, a)$  is usually referred to as *state-action value function* and each  $Q_{\pi}(s, a)$  regarding different policy  $\pi$  has a finite convergence value, which make it concrete to find  $Q_{\pi^*}(s, a)$ . And as long as we know about  $Q_{\pi^*}(s, a)$ , we are allowed to derive the near-optimal policy  $\pi^*$  by Eq. (16). Moreover,  $Q_{\pi}(s, a)$  still conserves certain information, even after our discount of future reward: we discount much to the reward that might be obtained in the distant future but not that much to the near one, so it actually partially reveals the exact value of a station-action pair (i.e., the cumulative rewards that might gain in the future). Actually, we can state that  $\pi^* \approx \tilde{\pi}^*$ . Later in our analysis, we would alternatively search for  $\pi^*$  as our target.

To derive  $Q_{\pi^*}(s, a)$ , we need to notice that:

$$Q_{\pi^*}(s, \pi^*(s)) = \max_{a \in \mathcal{A}_s} Q_{\pi^*}(s, a) \quad (17)$$

The above result follows our definition of  $\pi^*$  in Eq. (16).

Besides, as per Eq. (15),  $Q_{\pi}(s, a)$  can indeed rewrite to the following form:

$$\begin{aligned} & Q_{\pi}(s, a) \\ &= \mathbb{E}_{s_2} [r(s_1, a_1) + \beta Q_{\pi}(s_2, \pi(s_2)) \mid s_1 = s, a_1 = a] \end{aligned} \quad (18)$$

Plugging  $\pi^*$  into Eq. (18), it yields:

$$\begin{aligned} & Q_{\pi^*}(s, a) \\ &= \mathbb{E}_{s_2} [r(s_1, a_1) + \beta Q_{\pi^*}(s_2, \pi^*(s_2)) \mid s_1 = s, a_1 = a] \end{aligned} \quad (19)$$



And plugging Eq. (17) into Eq. (19), we have:

$$Q_{\pi^*}(s, a) = \mathbb{E}_{s_2} \left[ r(s_1, a_1) + \beta \max_{a_2 \in \mathcal{A}_{s_2}} Q_{\pi^*}(s_2, a_2) \mid s_1 = s, a_1 = a \right] \quad (20)$$

As per the **Markov** and **temporally homogeneous** property of an SMDP, we have:

$$Q_{\pi^*}(s, a) = \mathbb{E}_{s'} \left[ r(s, a) + \beta \max_{a' \in \mathcal{A}_{s'}} Q_{\pi^*}(s', a') \right] \quad (21)$$

where  $s'$  is a random variable (r.v.), which represents the next state that current state  $s$  will transfer to. This equation is called *Bellman optimality* and it indeed specifies the value of taking a specific action, which is basically composed of two parts:

- 1) The first part is the expected reward that is immediately obtained after actions have been taken, embodied by  $\mathbb{E}[r(s, a)]$ .
- 2) The second part is the discounted future expected rewards after the action has been taken, embodied by  $\mathbb{E}[\beta \max_{a' \in \mathcal{A}_{s'}} Q_{\pi^*}(s', a')]$ . This literally addresses challenge 5) **Coupling effects of actions between requests** we proposed below *P2*. The coupling effects are in fact embodied by these discounted expected rewards: by taking a different action, the state might experience a different transfer probability and thereby making the future rewards being affected. By this MDP formulation, we are enabled to have a concrete model of this coupling effect to the future.

Besides, specified by the proposed challenges below *P2*, we know that both the energy and request arrival pattern, as well as the data size distribution, are all unknown to the scheduler, which means that it is hopeless to derive the closed-form  $Q_{\pi^*}(s, a)$ . More explicitly, since the state transferred probability  $p(s'|s, a)$  (or  $p(s_{i+1}|s_i, a_i)$  in Eq. (12)) is an unknown constant, we cannot expand the expectation in Eq. (21), making  $Q_{\pi^*}(s, a)$  unachievable in an analytical way. Without knowledge of  $Q_{\pi^*}(s, a)$ , we are unable to fulfill our ultimate goal, i.e., to derive  $\pi^*$ .

Fortunately, there still exists an alternative path to derive  $Q_{\pi^*}(s, a)$ . (Henceforth, we use  $Q(s, a)$  to denote  $Q_{\pi^*}(s, a)$  for sake of brevity). If we have sufficient amount of data over a specific state and action (captured by a set  $X_{s,a}$ ), each piece of which shapes like this 4-element tuple:  $x \triangleq (s, a, r(s, a), s')$ , then we can estimate  $Q(s, a)$  by:

$$Q(s, a) \approx \frac{1}{|X_{s,a}|} \sum_{x \in X_{s,a}} \left[ r(s, a) + \beta \max_{a' \in \mathcal{A}_{s'}} Q(s', a') \right] \quad (22)$$

where  $|\cdot|$  returns the cardinality of a set. Or we aim to minimize the *estimation error*, i.e., to minimize the following term:

$$\frac{1}{|X|} \sum_{x \in X} \left[ Q(s, a) - \left( r(s, a) + \beta \max_{a' \in \mathcal{A}_{s'}} Q(s', a') \right) \right]^2 \quad (23)$$

where  $X = X_{s_1, a_1} \cup \dots \cup X_{s_1, a_n} \cup \dots$  captures all the available data. In this way, we do not need prior knowledge about the transferred probability i.e.,  $p(s'|s, a)$ , but we learn

it from the real state transferred data. This learning-based method completely resolves the **unknown distribution issues** we raised below *P2*.

Unfortunately, this initial idea is still unworkable. The major impediment is that there are **infinite amount of states** in our formulated problem! We simply cannot iteratively achieve  $Q(s, a)$  for every possible state-action pair, but at least, this initial idea points out a concrete direction that elicits our later double deep Q network solution.

### 4.3 A Double Deep Q Network Solution

In the previous section, we provide an initial idea about how to derive  $Q(s, a)$  in a learning way. But we simply cannot record  $Q(s, a)$  for each state due to the unbounded state space. This hidden issue motivates us to use a neural network to predict the optimal state-action value (abbreviated as *Q value* henceforth). Explicitly, we input a specific state to the neural network and output the Q value for action 1 to  $n$ . By this means, we do not need to record the Q value, but it is estimated based on the output after going through the neural network.

Formally, the estimated Q value can be denoted by  $Q(s, a; \theta_i)$  where  $\theta_i$  denotes the parameters of the neural network (termed Q network henceforth) after  $i$  steps of training. And following the same idea we proposed before, we expect to minimize the estimation error (or *loss* henceforth), in this form:

$$L_i(\theta_i) = \frac{1}{|\tilde{X}_i|} \sum_{x \in \tilde{X}_i} \left[ Q(s, a; \theta_i) - \left( r(s, a) + \beta \max_{a' \in \mathcal{A}_{s'}} Q(s', a'; \theta_i) \right) \right]^2 \quad (24)$$

where  $\tilde{X}_i$  is a sub-set of total available data when doing training for the  $i$ -th step, which is often referred to as *mini-batch*. We introduce such a concept here since the data acquiring process is an online process. In other words, we do not have all the training data naturally, but we obtain it through continuous interaction (i.e., acting action) and continuous policy update. As a result of this continuous update of data, it is simply not "cost-effective" to involve all the historical data we currently have in every step of training. As a refinement, only a subset of the data, i.e.,  $\tilde{X}_i$  is involved in the loss back-propagating for each step of training.

However, the above-defined loss, though is quite intuitive, would possibly lead to training instability of the neural network, since it is updated too radically (see [14]). As per [13], a double network solution would ensure a more stable performance. In this solution, we introduce another network, known as *target network*, whose parameters are denoted by  $\theta_i^-$ . The target network has exactly the same network architecture as the Q network and its parameters would be overridden periodically by the Q network. Informally, it serves as a "mirror" of the past Q network, which significantly reduces the training variation of the current Q network. The re-written loss function after adopting the double network architecture can be viewed in Eq. (25) (located at the top of the next page).

Now we shall formally introduce our proposed solution termed Neural network-based Adaptive Frequency

$$L_i(\theta_i) = \frac{1}{|\tilde{X}_i|} \sum_{x \in \tilde{X}_i} \left[ Q(s, a; \theta_i) - \left( r(s, a) + \beta Q \left( s', \arg \max_{a' \in \mathcal{A}_{s'}} Q(s', a'; \theta_i); \theta_i^- \right) \right) \right]^2 \quad (25)$$

where  $\theta_i^-$  denotes the parameters of target network.

---

**Algorithm 1** Training Stage of NAFA
 

---

*Input:*

Initial/minimum exploration factor,  $\epsilon_0 / \epsilon_{min}$ ;  
 Discount factor for rewards/exploration factor,  $\beta / \xi$ ;  
 Tradeoff Parameter,  $\eta$ ; Learning rate  $\gamma$ ;  
 Update periodicity of target network,  $\zeta$ ;  
 Steps per episode,  $N_{max}$ ; Training episodes,  $ep_{max}$ ;  
 Batch size,  $|\tilde{X}_i|$ ; Memory size,  $X_{max}$ ;

*Output:*

After-trained network parameters;  $\theta_{final}$

```

1: Initialize  $\theta_i$  and  $\theta_i^-$  with arbitrary values
2: Initialize  $i = 1, \epsilon = \epsilon_0$ 
3: Initialize empty replay memory  $X$ 
4: Initialize environment (or system status)
5: for  $ep \in \{1, 2, \dots, ep_{max}\}$  do
6:   Wait until the first request comes
7:   repeat
8:     Observe current system status  $s$ 
9:     if  $\text{random}() < \epsilon$  then
10:      Randomly select action  $a$  from  $\mathcal{A}_s$ 
11:     else
12:        $a = \arg \max_{a \in \mathcal{A}_s} Q(s, a; \theta_i)$ 
13:     end if
14:     Perform action  $a$  and realize reward  $r(s, a)$ 
15:     Wait until the next request comes
16:     Observe current system status  $s'$ 
17:     Store  $(s, a, r(s, a), s')$  into replay memory  $X$ 
18:     Sample minibatch  $\tilde{X}_i \sim X$ 
19:     Update parameter  $\theta_{i+1}$  following
           
$$\theta_{i+1} = \theta_i - \gamma \nabla_{\theta_i} L_i(\theta_i) \quad (26)$$

20:      $\epsilon_i = \epsilon_{min} + (\epsilon_0 - \epsilon_{min}) \cdot \exp(-i/\xi)$ 
21:     if  $i \bmod \zeta = 0$  then
22:        $\theta_{i+1}^- = \theta_{i+1}$ 
23:     else
24:        $\theta_{i+1}^- = \theta_i^-$ 
25:     end if
26:      $i = i + 1$ 
27:   until  $i > ep \cdot N_{max}$ 
28:   Reset the environment (or system status)
29: end for
30:  $\theta_{final} = \theta_i$ 

```

---

Adjustment (NAFA), whose running procedure on training and application stage are respectively shown in Algorithm 1 and Algorithm 2. Overall, the running procedure of NAFA can be summarized as follows:

- 1) **Initialization:** NAFA first initializes the Q network with arbitrary values and set the exploration factor to a pre-set value.
- 2) **Iterated Training:** We divide the training into sev-

eral episodes of training. The environment (i.e., the system status) will be reset to the initial stage each time an episode ends. In each episode, after the first request comes, the following sub-procedures perform in sequence:

- a) **Schedule Action:** NAFA observes the current system status  $s$  (or state in our MDP formulation). Targeting the to-be scheduled request (i.e., the  $i$ -th request), NAFA adopts a  $\epsilon$ -greedy strategy. Explicitly, with probability  $\epsilon$ , NAFA randomly explores the action space and randomly selects an action. With probability  $1 - \epsilon$ , NAFA greedily selects action based on the current system status  $s$  and the current Q network's output.
- b) **Interaction:** NAFA performs the decided action  $a$  within the **environment**. A corresponding reward would be realized as per Eq. (11). Note that the **environment** here could be real **operation environment** of a MEC server, or could be a **simulation environment** that is set up for a training purpose.
- c) **Data Integration:** After the interaction, NAFA sleeps until a new request has arrived. Once evoked, NAFA checks the current status  $s'$  (regarded as next state in the current iteration) and stores it into *replay memory* collectively with current state  $s$ , action  $a$ , and realized reward  $r(s, a)$ . The replay memory has a maximum size  $X_{max}$ . If the replay memory goes full, the oldest data will be replaced by the new one.
- d) **Update Q Network:** A fixed batch size of data is sampled from replay memory to the minibatch  $\tilde{X}_i$ . Then, NAFA performs back-propagation with learning rate  $\gamma$  on the Q network using samples within minibatch  $\tilde{X}_i$  and the loss function defined in Eq. (25).
- e) **Update Exploration Factor and Target Q Network:** NAFA discounts  $\epsilon$  using a discount factor  $\xi$  and update the target network at a periodicity of  $\zeta$  steps. After that, NAFA starts a new training iteration.

- 3) **Application:** After training has finished (i.e., it has gone through  $ep_{max} \cdot N_{max}$  steps of training), the algorithm uses the obtained Q network (whose parameters denoted by  $\theta_{final}$ ) to schedule requests in the real **operation environment**, i.e., based on current state  $s_i$ , action  $a_i = \arg \max_{a \in \mathcal{A}_{s_i}} Q(s_i, a; \theta_{final})$  will be taken for each request.

**Algorithm 2** Application Stage of NAFA

---

*Input:*  
After-trained network parameters;  $\theta_{final}$

*Output:*  
Action sequence;  $a_1, a_2, \dots$

- 1:  $i = 1$
- 2: **for** each request comes **do**
- 3:   Observe system status  $s_i$
- 4:    $a_i = \operatorname{argmax}_{a \in \mathcal{A}_s} Q(s_i, a; \theta_{final})$
- 5:   Perform action  $a_i$
- 6:    $i = i + 1$
- 7: **end for**

---

**5 EXPERIMENT****5.1 Setup****5.1.1 Basic setting**

- **Programming and running environment:** We have implemented NAFA and the simulation environment on the basis of PyTorch and gym (a site package that is commonly used for environment construction in RL). Besides, all the computation in our simulation is run by a high-performance workstation (Dell PowerEdge T630 with 2xGTX 1080Ti).
- **Simulation of energy arrival:** In our simulation, NAFA is deployed on an MEC server which is driven by solar power (a typical example of intermittent energy supply). To simulate the energy arrival pattern, we use the data from HelioClim-3<sup>4</sup>, a satellite-derived solar radiation database. Explicitly, we derive the Global Horizontal Irradiance (GHI) data in Kampala, Uganda (latitude 0.329, longitude 32.499) from 2005-01-01 to 2005-12-31 (for train dataset) and 2006-01-01 to 2006-12-31 (for test dataset). Note that the GHI data in some days are missing in the dataset, so we use 300 out of 365 days of intact data respectively from the train and test dataset during our experiment. By the GHI data, we calculate the amount of arrival energy during a given time interval  $[t_1, t_2]$ , as the following form:

$$\lambda_{t_1, t_2} = \int_{t_1}^{t_2} \text{panel\_size} \cdot \text{GHI}(t) dt \quad (27)$$

where `panel_size` is the solar panel size of an MEC server. By  $\lambda_{t_1, t_2}$ , we can derive the energy arrival between two request arrivals, i.e.,  $\lambda_{i, i+1}$ .

- **Simulation of request arrival and data size:** We use a Poisson process (with arrival rate  $\lambda_r$ ) to generate the request arrival events (similar simulation setting available in [15], [16]). The data size of the request follows a uniform distribution (similar setting available in [17], [18]) in the scale of 10MB to 30MB, i.e.,  $d_i \sim \text{Uniform}(10, 30)$  MB.
- **Action space:** We consider 4 possible actions for each request (i.e., three correspond to different levels of frequency and one is rejection action). Formally, for the  $i$ -th request,  $a_i \in \{0, 1, 2, 3\}$ , where

4. <http://www.soda-pro.com/web-services/radiation/helioclim-3-archives-for-free>

TABLE 2: Simulation parameters

Symbols	Meanings	Values
$\nu$	computation complexity	2e4
$\kappa$	effective switched capacitance	1e-28
$m$	number of CPU cores	12
$B_{max}$	battery capacity	1e6 (Joules)
<code>panel_size</code>	solar panel size	0.5 ( $m^2$ )

TABLE 3: Training hyper-parameters for NAFA

Symbols	Meanings	Values
$\epsilon_0$	initial exploration factor	0.5
$\epsilon_{min}$	minimum exploration factor	0.01
$\xi$	discount factor for exploration	3e4
$\gamma$	learning rate	5e-4
$\beta$	discount factor for rewards	0.995
$\zeta$	target network update periodicity	5000
$ \bar{X}_i $	batch size	80
$X_{max}$	size of replay buffer	1e6

actions  $\{1, 2, 3\}$  correspond to processing frequency  $\{2, 3, 4\}$ GHz and action 0 induces request rejection.

- **Network Structure:** The target network and Q network in NAFA have exactly the same structure: a Deep Neural Network (DNN) model with two hidden layers, each with 200 and 100 neurons, activated by ReLu, and an output layer, which outputs the estimated Q value for all 4 actions.
- **Simulation parameters:** All of the simulation parameters have been specified in Table 2.
- **Hyper-parameters and training details of NAFA:** All hyper-parameters are available in Table 3. In our simulation, we use  $ep_{max} = 30 \times 5$  episodes to train the model. The simulation time for each episode of training is 10 straight days. We reset the simulation environment based on different GHI data once the last request within these 10 days has been scheduled.<sup>5</sup> Besides, it is important to note that, since we only have  $30 \times 10$  days of GHI data as our training dataset, we re-use the same  $30 \times 10$  days of GHI data for training episodes between  $30 \times 2$  to  $30 \times 5$ .
- **Uniformization of states:** In our implementation of NAFA, we have uniformed all the elements' values in a state to the scale of  $[0, 1]$  before its input to the neural network. We are prone to believe that such a uniformization might potentially improve the training performance.

**5.1.2 Baselines**

For an evaluation purpose, we implement three baseline methods, specified as follows:

- 1) **Best Fit (BF):** Best Fit is a rule-based scheduling algorithm derived from [19]. In our problem, BF tends to reserve energy for future use by scheduling the

5. So, in our real implementation, training steps  $N_{max}$  is not necessarily identical for all the training episodes.

minimized processing frequency for the incoming request. Explicitly, it selects an action:

$$a_i = \begin{cases} \operatorname{argmin}_{a \in \mathcal{A}_{s_i}} f_a & |\mathcal{A}_{s_i}| > 1 \\ 0 & \text{otherwise} \end{cases} \quad (28)$$

- 2) **Worst Fit (WF):** Worst Fit is another rule-based scheduling algorithm derived from [20]. In our problem, WF is desperate to reduce the processing time of each request. It achieves this goal via scheduling the maximized processing frequency for the incoming request as far as it is possible. Explicitly, it selects an action:

$$a_i = \begin{cases} \operatorname{argmax}_{a \in \mathcal{A}_{s_i}} f_a & |\mathcal{A}_{s_i}| > 1 \\ 0 & \text{otherwise} \end{cases} \quad (29)$$

- 3) **linUCB:** linUCB is an online learning solution and it is typically applied in a linear contextual bandit model (see [21]). In our setting, linUCB learns the immediate rewards achieved by different contexts (or states in our formulation) and it greedily selects the action that maximizes its estimated immediate rewards. However, it disregards the state transfer probability, or in other words, it ignores the rewards that might be obtained in the future. Besides, same as NAFA, in our implementation of linUCB, we perform the same uniformization process for a state before its training. We do this in a bid to ensure a fair comparison.

In our experiment, we train linUCB and NAFA for the same amount of episodes. After training, we use 300 straight days of simulation based on the same test dataset to validate the performance of different scheduling strategies.

## 5.2 Results

### 5.2.1 Tradeoff vs. Average Rewards

With the request arrival rate fixing to  $\lambda_r = 30$  and different settings of tradeoff parameters  $\eta$ , we shall show how different scheduling strategies work. The results can be viewed in the box plot, shown in Fig. 3. From this plot, we can derive the following observations:

- 1) In all the settings of  $\eta$ , NAFA outperforms all the other baselines in terms of average returned rewards. This result strongly shows the superiority of our proposed solution: not only is NAFA capable of adaptively adjusting its action policy based on the operator's preference (embodied by tradeoff  $\eta$ ), but it also has a stronger learning performance, comparing with another learning algorithm, i.e., linUCB.
- 2) With  $\eta$  becoming bigger, NAFA and linUCB's average rewards approach to 0 while other rule-based algorithms (i.e., WF and BF) reduce to a negative number. Our explanation for this phenomenon is that when  $\eta$  is set to a sufficiently high value, the penalty brought by processing time has exceeded the real rewards brought by accepting a request (see our definition of rewards in Eq.(11)). As such, accepting a request which takes too much time to process, is no longer a beneficial action for this

extreme tradeoff setting, so both NAFA and linUCB learn to only accept a small portion of requests (perhaps those with smaller data size) and only acquire a slightly positive reward.

### 5.2.2 Processing Time vs. Rejection Ratio

Recall that the reward is exactly composed of two parts: real reward of accepting a request, and a penalty of processing time. To draw a clearer picture of these two parts, we show in Fig. 4 how different algorithms (and in a different setting of  $\eta$ ) perform in terms of processing time and rejection ratio when fixing  $\lambda_r = 30$ . Intuitively, we derive the following observations:

- 1) Comparing BF with WF, BF leads to a higher average processing time, but meanwhile, a lower average rejection ratio is also observed. This phenomenon is wholly comprehensible if considering the working pattern of BF and WF. BF tends to schedule the incoming request to a lower processing frequency in an attempt to conserve energy for future use. This conserved action might lead to a higher average processing time. But at the same time, it is supposed to have a lower rejection ratio when the power supply is limited (e.g. at nights). By contrast, WF might experience more rejection due to power shortage at this time, as a result of its prodigal manner.
- 2) With a larger tradeoff  $\eta$ , NAFA and linUCB experience a drop in terms of processing latency, but a rise in the rejection ratio is also observed. It again corroborates that the tradeoff parameter  $\eta$  defined in rewards is functioning well, meeting the original design purpose. In this way, operators should be able to adaptively adjust the algorithm's performance based on their own appetites towards the two objectives.
- 3) NAFA-0, NAFA-1, and NAFA-2 significantly outperform BF in terms of both the two objectives, i.e., smaller processing time and lower rejection ratio. Besides, NAFA-2 and NAFA-3 also outperform WF. Of the same tradeoff parameter, linUCB is outperformed by NAFA in terms of both the two objectives in most of the experiment groups. Finally, not an algorithm outperforms NAFA in both the objectives. These observations further justified the superiority of NAFA.

### 5.2.3 Analysis of Request Treatment and Rejection Motivation

To have a closer inspection on the algorithms' performance and to explore the hidden motivation that leads to rejection, by Fig. 5, we show the composition of requests treatment while again fixing  $\eta = 30$ . Based on the figure, the following observations follow:

- 1) Most of the rejections of WF is caused by energy full-reserved while most of the rejections of BF is resulting from resource full-loaded. This phenomenon is in accordance with their respective behavioral pattern. BF, which is thrifty on energy usage, might experience too-long processing time, which in turn

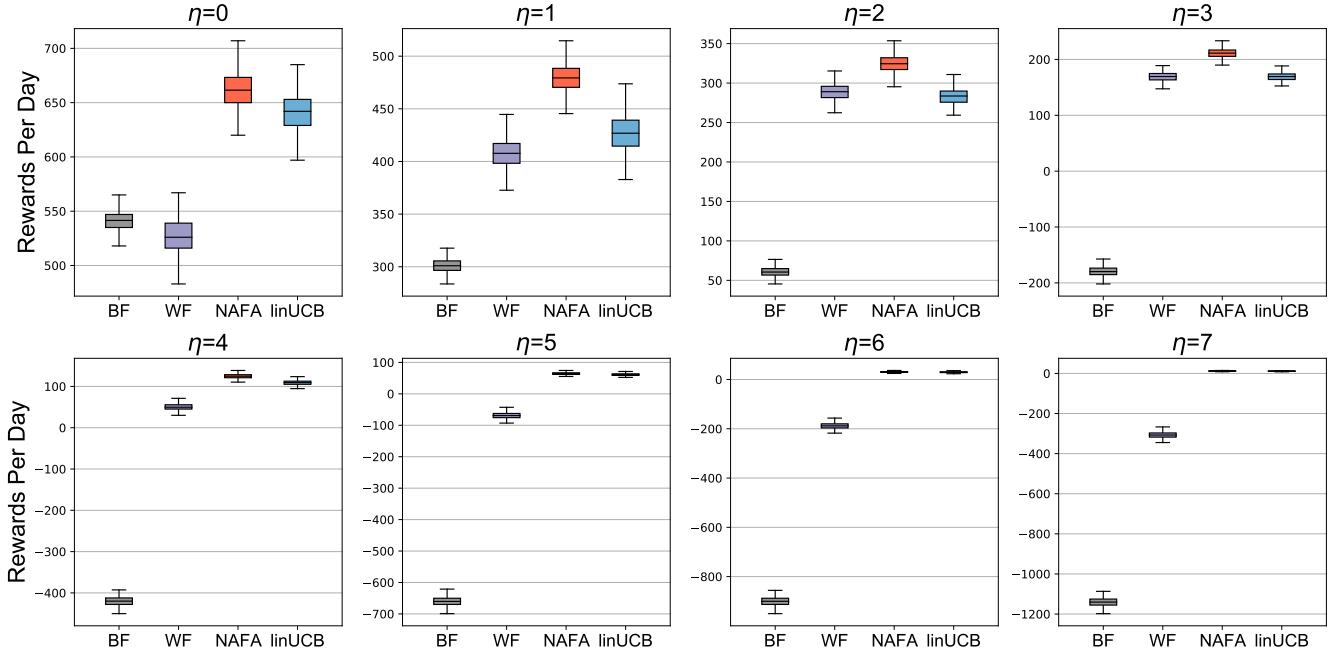


Fig. 3: Box plot demonstrating rewards per day vs. tradeoff  $\eta$  fixing  $\lambda_r = 30$ . Each of the sub-figures demonstrates reward data of 300 straight simulation days, using the same testing dataset.

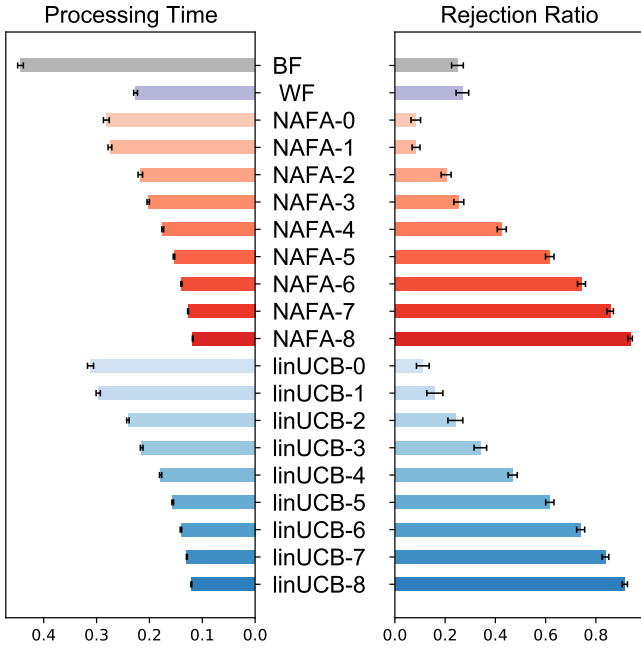


Fig. 4: Processing time vs. rejection ratio when fixing  $\lambda_r = 30$ . NAFA-**number** and linUCB-**number** are used to denote different values of  $\eta$  setting during the training of NAFA and linUCB, respectively.

leads to unnecessary rejection when all the CPU cores are full (i.e., resource full-loaded). By contrast, a prodigal usage of energy might bring about energy full-reserved, as WF is experiencing.

- 2) linUCB and NAFA are able to balance the trade-off between resource full-loaded and energy full-

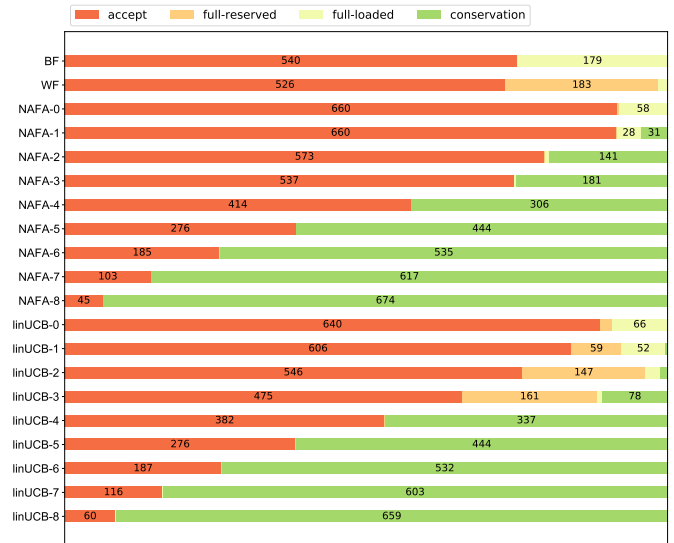


Fig. 5: Composition of request treatment and rejection motivations for different algorithms when fixing  $\lambda_r = 30$ . We assume the rejections is led by **full-reserved** when energy in the battery has mostly be reserved, so there is no action can be taken. Analogously, the requests are rejected by the **full-loaded** when all the free CPU cores are exhausted (in a rare case that the server is simultaneously full-loaded and full-reserved, we count it as full-reserved). Request rejected due to neither of the reasons will be counted as **conservation** purpose.

TABLE 4: Experimental data under the setting of different tradeoff parameters  $\eta$  and a fixed request arrival rate  $\lambda_r = 30$ . The data of the highest acceptance, the lowest average processing time, and the highest average rewards among the same group of experiment have been highlighted.

Tradeoff	Methods	Average Request Treatment and Rejection Motivations				Average Processing time	Average Rewards
		Accept	Full-reserved	Full-loaded	Conservation		
$\eta = 0$	BF	540.96	0.40	179.71	0.00	0.333	540.96
	WF	526.90	183.12	11.04	0.00	<b>0.165</b>	526.90
	NAFA	<b>660.85</b>	1.97	58.07	0.17	0.258	<b>660.85</b>
	linUCB	640.52	14.00	66.55	0.00	0.277	640.52
$\eta = 2$	BF	540.96	0.40	179.71	0.00	0.333	60.72
	WF	526.90	183.12	11.04	0.00	<b>0.165</b>	288.58
	NAFA	<b>573.66</b>	0.42	5.60	141.38	0.173	<b>324.49</b>
	linUCB	546.96	147.86	16.82	9.42	0.183	283.61
$\eta = 4$	BF	<b>540.96</b>	0.40	179.71	0.00	0.333	-419.51
	WF	526.90	183.12	11.04	0.00	0.165	50.27
	NAFA	414.16	0.40	0.04	306.46	0.100	<b>124.66</b>
	linUCB	382.85	0.40	0.11	337.70	<b>0.095</b>	109.06
$\eta = 6$	BF	<b>540.96</b>	0.40	179.71	0.00	0.333	-899.75
	WF	526.90	183.12	11.04	0.00	0.165	-188.05
	NAFA	185.50	0.40	0.00	535.16	<b>0.036</b>	<b>30.25</b>
	linUCB	187.80	0.40	0.00	532.87	0.037	29.59
$\eta = 8$	BF	<b>540.96</b>	0.40	179.71	0.00	0.333	-1379.99
	WF	526.90	183.12	11.04	0.00	0.165	-426.37
	NAFA	45.87	0.40	0.00	674.80	<b>0.008</b>	<b>2.50</b>
	linUCB	60.98	0.40	0.00	659.68	0.010	2.09

loaded, and thereby, resulting in an increase in the overall request acceptance ratio.

- 3) With  $\eta$  becoming larger, both linUCB and NAFA develop a conservation action pattern: some requests are deliberately rejected when no resource full-loaded or energy full-loaded is experiencing. There are two explanations for this pattern: the first is that a) penalty brought by processing latency exceeds the rewards brought by acceptance, even if the action with the highest frequency is taken. Then there is simply no benefit to accept such a request (typically is a request with a large data size). The second motivation is b) the algorithm learns to reject some specific requests (perhaps those larger ones) if the system is nearly full-loaded and full-reserved. Apparently, the conservation pattern that linUCB develops is mostly based on the first motivation, as it has no regard on the state transfer (or informally, the future), while the SMDP-based NAFA should be able to learn both of the two motivations. In addition, corroborated by Fig. 3, the "prophetic" NAFA could indeed gain us more rewards and therefore substantiate the necessity of full consideration of both the two motivations.

To gain us a more accurate observation, we demonstrate the average request treatment data in Table 4.

#### 5.2.4 Rewards vs. Request Arrival Rate

In this experiment, we fix the tradeoff parameter to  $\eta = 0$  and  $\eta = 3$ , and see how the returned rewards evolve with the change of request arrival rate  $\lambda_r$ . By Fig. 6, we find that:

- 1) Fixing tradeoff  $\eta = 0$ , all the algorithms experience a rise in rewards with the growth of request arrival

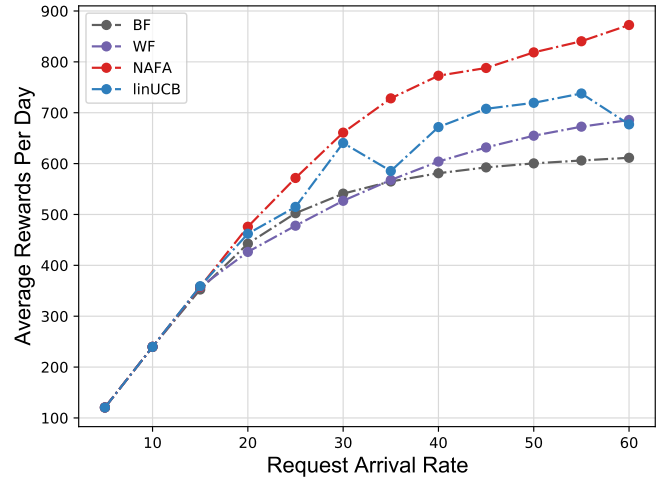


Fig. 6: Average Rewards vs. Request Arrival Rate when fixing tradeoff parameter  $\eta = 0$

rate. This phenomenon is quite comprehensible since every single request brings positive rewards (a constant 1 when  $\eta = 0$ ) if being properly scheduled.

- 2) However, the growth of WF and BF stagnates as the arrival rate becomes really big. By contrast, NAFA seems to continuously increase in the acquired rewards. By this observation, we see that the traditional rule-based algorithms apparently are incompetent of meeting the scheduling requirement when the system is in a high-loaded status.
- 3) linUCB experiences a drastic jitter under different request arrival rates. We speculate that this jitter is

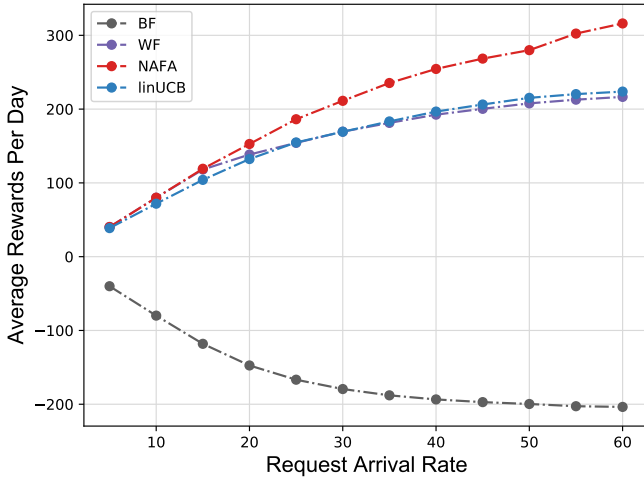


Fig. 7: Average Rewards vs. Request Arrival Rate when fixing tradeoff parameter  $\eta = 3$

resulting from a constant reward achieved for every state (or context). When  $\eta = 0$ , the algorithm simply reduces to a random selection since each action has exactly the same expected rewards for almost all the states (except those when the system is full-loaded or full-reserved).

By Fig. 7, we also find that, for  $\eta = 3$ :

- 1) BF gained a negative average reward. This is resulting from the excessively high processing time penalty if only employing the least processor frequency.
- 2) NAFA again acquires the highest average reward in all groups of experiments.

### 5.2.5 Acceptance Ratio and Processing Time vs. Request Arrival Rate

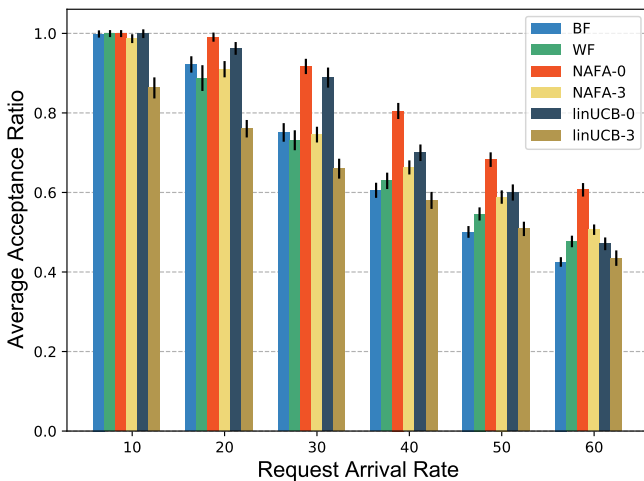


Fig. 8: Average acceptance ratio vs. request arrival rate. NAFA-Number and linUCB-Number represent the algorithms trained in the setting of  $\eta = \text{Number}$ .

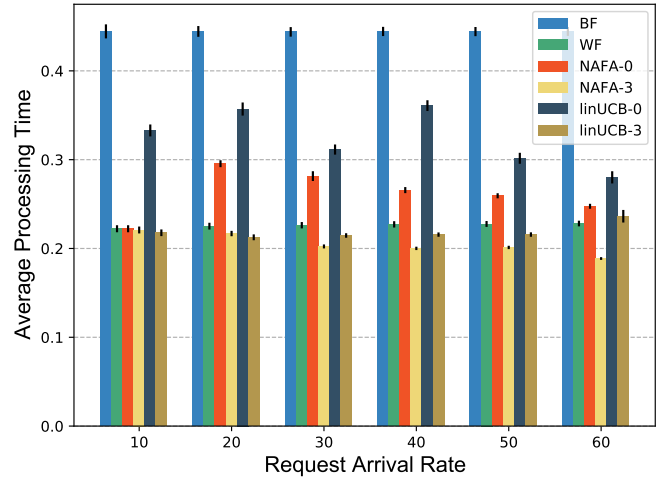


Fig. 9: Average processing time vs. request arrival rate. NAFA-Number and linUCB-Number represent the algorithms trained in the setting of  $\eta = \text{Number}$ .

To show the whole picture, we now demonstrate in Fig. 8 and Fig. 9 how the two objectives, i.e., acceptance ratio and processing time evolve with different request arrival rates. Based on the result, we give the following observations:

- 1) Processing time of BF and WF shows little variation with request arrival rate. This phenomenon is intuitive since these rule-based methods are prone to schedule the same frequency to the incoming request (the largest one for WF and the smallest one for BF).
- 2) Compared to WF, BF acquires a higher acceptance ratio when the request rate is relatively low, but WF surpasses BF when the request rate becomes greater. Obviously, this phenomenon seems to be telling us that when the request rate is sufficiently high, the system is more vulnerable to resource full-loaded than to energy full-reserved.
- 3) NAFA-0 yields the largest acceptance ratio while NAFA-3 yields the smallest processing time, comparing to other baselines. This corroborates the effectiveness and high adaptiveness of NAFA.
- 4) linUCB-0 acquires the second-largest acceptance ratio and linUCB-3 acquires the second-smallest processing time. This substantiates some sort of adaptiveness of linUCB. However, its performance could not match up with NAFA due to its "near-sighted" action pattern.

To enable an accurate observation, we demonstrate in Table 5 our experimental data given different request arrival rate and a fixed tradeoff parameter  $\eta = 3$ .

## 6 CONCLUSION AND FUTURE PROSPECT

In this paper, we have studied an adaptive frequency adjustment problem in the scenario of intermittent energy supplied MEC. Concerning multiple tradeoffs persisted in the formulated problem, we propose a deep reinforcement learning-based solution termed NAFA for problem-solving.



TABLE 5: Experimental data under the setting of different request arrival rates  $\lambda_r$ , and a fixed tradeoff parameter  $\eta = 3$ . The data of the highest acceptance, the lowest average processing time and the highest average rewards among the same group of experiment have been highlighted.

Request Arrival Rate	Methods	Average Request Treatment and Rejection Motivations				Average Porcessing time	Average Rewards
		Accept	Full-reserved	Full-loaded	Conservation		
$\lambda_r = 10$	BF	239.57	0.12	0.24	0.00	0.444	-79.90
	WF	<b>239.82</b>	0.12	0.00	0.00	0.222	<b>79.93</b>
	NAFA	236.74	0.12	0.00	3.07	0.218	79.91
	linUCB	206.95	0.12	0.00	32.86	<b>0.188</b>	71.82
$\lambda_r = 20$	BF	<b>442.60</b>	0.26	37.58	0.00	0.409	-147.45
	WF	426.40	53.52	0.51	0.00	0.200	138.41
	NAFA	437.04	0.31	0.26	42.83	0.197	<b>152.73</b>
	linUCB	365.21	0.26	0.13	114.84	<b>0.162</b>	132.32
$\lambda_r = 30$	BF	<b>540.96</b>	0.40	179.71	0.00	0.333	-179.40
	WF	526.90	183.12	11.04	0.00	0.165	169.42
	NAFA	537.32	0.42	2.21	181.12	0.151	<b>211.24</b>
	linUCB	475.40	161.54	5.87	78.26	<b>0.141</b>	169.32
$\lambda_r = 40$	BF	581.07	0.51	379.01	0.00	0.269	-193.47
	WF	603.99	303.22	53.38	0.00	0.143	192.47
	NAFA	<b>636.54</b>	9.50	13.54	301.01	0.133	<b>254.44</b>
	linUCB	556.83	280.75	35.30	87.72	<b>0.125</b>	196.66
$\lambda_r = 50$	BF	600.43	0.67	598.87	0.00	0.222	-199.66
	WF	654.79	415.44	129.74	0.00	0.124	207.77
	NAFA	<b>705.85</b>	23.46	33.11	437.55	0.118	<b>279.90</b>
	linUCB	609.75	390.90	96.49	102.82	<b>0.110</b>	215.26
$\lambda_r = 60$	BF	611.44	0.79	826.66	0.00	0.189	-203.62
	WF	685.65	522.45	230.79	0.00	0.109	216.56
	NAFA	<b>728.35</b>	23.83	33.79	652.92	<b>0.096</b>	<b>316.10</b>
	linUCB	625.43	506.13	186.60	120.73	0.103	223.75

By our real solar data-based experiments, we substantiate the adaptiveness and superiority of NAFA, which drastically outperforms other baselines in terms of acquired reward under different tradeoff settings.

For a potential extension of our proposed solution, we are particularly interested in a more advanced technique, known as Federated Learning (FL, [22]). FL allows multiple servers to collectively train a Deep Q network, while do not necessarily need to expose their private data to a centralized entity. This novel training paradigm is pretty advantageous over our extensions from the single-server to the multi-servers scenario: we might gain access to request and energy arrival patterns from different servers (perhaps in different venues and owned by different operators) without knowing its training data. With more diversified data being available for training, a more generalized neural network model might be obtained and could be put into real serving over millions (or billions) of self-powered micro MEC servers.

## REFERENCES

- [1] T. Huang, W. Lin, C. Xiong, R. Pan, and J. Huang, "An ant colony optimization-based multiobjective service replicas placement strategy for fog computing," *IEEE Transactions on Cybernetics*, pp. 1–14, 2020.
- [2] Z. Ning, P. Dong, X. Wang, M. S. Obaidat, X. Hu, L. Guo, Y. Guo, J. Huang, B. Hu, and Y. Li, "When deep reinforcement learning meets 5g vehicular networks: A distributed offloading framework for traffic big data," *IEEE Transactions on Industrial Informatics*, 2019.
- [3] H. Yang, A. Alphones, W.-D. Zhong, C. Chen, and X. Xie, "Learning-based energy-efficient resource management by heterogeneous rf/vlc for ultra-reliable low-latency industrial iot networks," *IEEE Transactions on Industrial Informatics*, 2019.
- [4] X. Li and X. Zhang, "Multi-task allocation under time constraints in mobile crowdsensing," *IEEE Transactions on Mobile Computing*, 2019.
- [5] C. H. Liu, Z. Dai, Y. Zhao, J. Crowcroft, D. O. Wu, and K. Leung, "Distributed and energy-efficient mobile crowdsensing with charging stations by deep reinforcement learning," *IEEE Transactions on Mobile Computing*, 2019.
- [6] X. Chen, H. Zhang, C. Wu, S. Mao, Y. Ji, and M. Bennis, "Performance Optimization in Mobile-Edge Computing via Deep Reinforcement Learning," *arXiv:1804.00514 [cs]*, Mar. 2018, arXiv: 1804.00514. [Online]. Available: <http://arxiv.org/abs/1804.00514>
- [7] Z. Wei, B. Zhao, J. Su, and X. Lu, "Dynamic Edge Computation Offloading for Internet of Things with Energy Harvesting: A Learning Method," *IEEE Internet of Things Journal*, pp. 1–1, 2019.
- [8] M. Min, X. Wan, L. Xiao, Y. Chen, M. Xia, D. Wu, and H. Dai, "Learning-Based Privacy-Aware Offloading for Healthcare IoT With Energy Harvesting," *IEEE Internet of Things Journal*, vol. 6, no. 3, pp. 4307–4316, Jun. 2019. [Online]. Available: <https://ieeexplore.ieee.org/document/8491311/>
- [9] M. Xu, A. N. Toosi, B. Bahrani, R. Razzaghi, and M. Singh, "Optimized renewable energy use in green cloud data centers," in *International Conference on Service-Oriented Computing*. Springer, 2019, pp. 314–330.
- [10] K. Zheng, H. Meng, P. Chatzimisios, L. Lei, and X. Shen, "An SMDP-Based Resource Allocation in Vehicular Cloud Computing Systems," *IEEE Transactions on Industrial Electronics*, vol. 62, no. 12, pp. 7920–7928, Dec. 2015.
- [11] M. Baljon, M. Li, H. Liang, and L. Zhao, "SMDP-Based Resource Allocation for Wireless Networks with Energy Harvesting Constraints," in *2017 IEEE 86th Vehicular Technology Conference (VTC-Fall)*, Sep. 2017, pp. 1–6.
- [12] L. Lei, H. Xu, X. Xiong, K. Zheng, and W. Xiang, "Joint Computation Offloading and Multi-User Scheduling using Approximate

- Dynamic Programming in NB-IoT Edge Computing System," *IEEE Internet of Things Journal*, pp. 1–1, 2019.
- [13] H. Van Hasselt, A. Guez, and D. Silver, "Deep reinforcement learning with double q-learning," in *Proceedings of the AAAI conference on artificial intelligence*, vol. 30, no. 1, 2016.
- [14] V. Mnih, K. Kavukcuoglu, D. Silver, A. A. Rusu, J. Veness, M. G. Bellemare, A. Graves, M. Riedmiller, A. K. Fidjeland, G. Ostrovski, S. Petersen, C. Beattie, A. Sadik, I. Antonoglou, H. King, D. Kumaran, D. Wierstra, S. Legg, and D. Hassabis, "Human-level control through deep reinforcement learning," *Nature*, vol. 518, no. 7540, pp. 529–533, Feb. 2015. [Online]. Available: <http://www.nature.com/articles/nature14236>
- [15] J. Xu, L. Chen, and S. Ren, "Online learning for offloading and autoscaling in energy harvesting mobile edge computing," *IEEE Transactions on Cognitive Communications and Networking*, vol. 3, no. 3, pp. 361–373, 2017.
- [16] Y. Mao, J. Zhang, and K. B. Letaief, "Dynamic computation offloading for mobile-edge computing with energy harvesting devices," *IEEE Journal on Selected Areas in Communications*, vol. 34, no. 12, pp. 3590–3605, 2016.
- [17] X. Lyu, W. Ni, H. Tian, R. P. Liu, X. Wang, G. B. Giannakis, and A. Paulraj, "Optimal schedule of mobile edge computing for internet of things using partial information," *IEEE Journal on Selected Areas in Communications*, vol. 35, no. 11, pp. 2606–2615, 2017.
- [18] Y. Chen, Y. Zhang, Y. Wu, L. Qi, X. Chen, and X. Shen, "Joint task scheduling and energy management for heterogeneous mobile edge computing with hybrid energy supply," *IEEE Internet of Things Journal*, 2020.
- [19] F. Farahnakian, T. Pahikkala, P. Liljeberg, J. Plosila, N. T. Hieu, and H. Tenhunen, "Energy-aware vm consolidation in cloud data centers using utilization prediction model," *IEEE Transactions on Cloud Computing*, 2016.
- [20] C. Xian, Y.-H. Lu, and Z. Li, "Energy-aware scheduling for real-time multiprocessor systems with uncertain task execution time," in *2007 44th ACM/IEEE Design Automation Conference*. IEEE, 2007, pp. 664–669.
- [21] W. Chu, L. Li, L. Reyzin, and R. Schapire, "Contextual bandits with linear payoff functions," in *Proceedings of the Fourteenth International Conference on Artificial Intelligence and Statistics*, 2011, pp. 208–214.
- [22] H. B. McMahan, E. Moore, D. Ramage, S. Hampson *et al.*, "Communication-efficient learning of deep networks from decentralized data," *arXiv preprint arXiv:1602.05629*, 2016.